Shahrood University of Technology
Iranian Society of Mining Engineering (IRSME)
Journal of Mining and Environment (JME)
journal homepage: www.jme.shahroodut.ac.ir
THOMSON REUTERS

Vol. 11, No. 1, 2020, 143-159.
*DOI: 10.22044/jme.2019.8709.1756*

# Geostatistical Modeling of Electrical Resistivity Tomography for Imaging Porphyry Cu Mineralization in Takht-e-Gonbad Deposit, Iran

M. Babaei, M. Abedi*, Gh.H. Norouzi and S. Kazem Alilou

*School of Mining Engineering, College of Engineering, University of Tehran, Tehran, Iran*

Received 17 July 2019; received in revised form 8 October 2019; accepted 19 October 2019

**Keywords**

*Electrical resistivity*

*Electrical chargeability*

*Geostatistics*

*Inversion*

*Porphyry Cu*

**Abstract**

In this work, the application of a geostatistical-based modeling approach is presented for building up the electrical properties acquired from a geophysical electrical tomography survey deployed for the purpose of porphyry Cu exploration at the Takht-e-Gonbad deposit in the central domain of Iran. The electrical data is inverted in 2D along several profiles across the main favorable zones of Cu-bearing mineralization to image the electrical resistivity and chargeability properties. Upon the tight spatial correlation of these geophysical properties and Cu mineralization (i.e. Cu grade), the electrical models are constructed in 3D through geostatistical interpolation of the 2D inverted data to provide insights into the geometry of the probable ore mineralization. The anomalous geophysical zone that coincides simultaneously with higher values of electrical chargeability and resistivity is in accordance with the main body of high Cu grades generated from exploratory drillings. It reveals that the porphyry-type Cu mineralization system in this area has strong geophysical footprints mainly controlled by rock types and alterations. These physical models supply valuable pieces of information for designing the layout of further exploratory drillings, constructing geological characteristics, separating non-mineralized zones form the mineralized zones, and resource modeling.

## 1. Introduction

Electrical survey is a part of popular geophysical methods employed to measure the electrical properties of bodies or rocks, especially to determine the measurable differences between rocks enriched or depleted by ore-bearing mineralization. Electrical geophysics can be used to delineate various sources of mineralization via measuring their electrical resistivity and chargeability [1]. Correct identification of contrasts arising from different physical properties of sought targets is the cornerstone of any geophysical method [2]. In many cases of mineral exploration, for amplifying the certainty of the acquired results, integration of several geophysical methods is genuinely unavoidable [3]. Due to optimization in cost and time of mineral exploration programs, the application of geophysical surveys has recently been increasing in the shallow and deep-seated ore-bearing investigations. As noted, the integrated geophysical methods are commonly used to obtain qualified results [4], where prevalent geophysical tools are induced polarization (IP) and resistivity (Res) for ores located in sulfide-bearing targets [5]. The main goal of the IP and Res methods is to localize the best drilling points for exploration purposes [6, 7].

A combination of electrical surveys has been widely and fruitfully carried out for various purposes in ore exploration, water and contamination studies, engineering and geological investigations, and so on. Among the numerous applications, we can mention polymetallic deposit delineation [8], waste management in hydrocarbon studies [9], porphyry copper mineralization [10, 11], manganese ore exploration [3], water studies [12, 13], Cu-dominated VHMS sulfate [4], Au-Ag deposit [14], oil bitumen [15], pollutant study of a

*Corresponding author: 2018maysamabedi@ut.ac.ir (M.Abedi).*

coal washing waste dump [16], delineation of acid rock drainage pathways in gold mine [17], Au-Cu mine tailings [18], contamination studies [19, 20], mineral alteration detection [21], and geological investigations for a landfill site [22, 7].

In most geoscience studies, interpolation is performed when the numerical modeling in a sparse-sampled area is required. However, the estimation techniques for a range of discrete sets of known data are examined. It means that the points between and around the available data would be estimated through interpolation techniques, categorized generally into the two main groups of classic statistical and geostatistical methods. The superiority of various geostatistical methods over the classical ones is that they take into account the spatial variability of the desired data to generate reliable spatial estimates along with the uncertainties arising from such estimates [23]. Note that the spatial correlation of data, which is controlled by distance and direction, can be incorporated in mathematical formulation to consider the spatial characteristics of the interpolated data. Among the interpolation techniques, spatial characteristics are usually searched through plotting a variogram model in geostatistics [24, 7].

Geostatistics was basically developed to estimate the sparse variables such as the grade of an ore body [25]. The geostatistical techniques have been examined in numerous geophysical studies for a variety of purposes [23-29], where the main aim has been to integrate the geophysical modeling and geostatistical interpolation for tackling problems arising from geological modeling. For instance, Abedi *et al*. (2015) [30] have incorporated the magnetic susceptibility property as a secondary soft and dense variable in the Fe-grade estimation when a very sparse pattern of drilling exists, the point that a remarkable spatial correlation has been observed between the first (hard) and second (soft) variables. In electrical geophysics, Asghari *et al*. (2016) [31] have employed multivariate geostatistics on electrical properties to estimate copper grade with lower amounts of the estimation variance and uncertainty. Meanwhile, a sulfide factor (as a ratio of the electrical chargeability to the electrical resistivity) has been calculated after inverse modeling of the electrical data to generate a correlated secondary variable for Cu grade estimates. The results obtained have verified that incorporating soft variable drastically outperforms the results over the cases of single variable estimates [31].

Since 3D modeling is more beneficial for designing the layout of exploratory drilling, the 3D representation of geophysical properties of electrical resistivity and chargeability can generate valuable pieces of information indirectly related to the geometry of a sought ore-bearing target [32]. In this research work, at first, the efficiency and applicability of the IP and Res surveys were investigated at the Takht-e-Gonbad Porphyry Cu Deposit (in the central domain of Iran) in detailed exploration and mining phase, whereby geophysical surveying was deployed along twelve 2D profiles with a configuration of pole-dipole array. For this purpose, 2D cross-sections of the IP and Res models were prepared for each profile by inverting the data through the approach proposed by Loke (2004) [33]. The spatial correlation between the electrical properties and Cu mineralization was checked out using exploratory boreholes, showing a meaningful amount of correlation among the physical properties and Cu grade. Constructing electrical properties in 3D was done by the SGeMS software (an open-source program), where the 3D models were interpolated from 2D electrical surveying and a sparse pattern of exploratory drilling. The results obtained indicated that geophysical models could appropriately lead to localization of the main body of Cu mineralization along with separating non-mineralized zones form the favorable mineralized zones.

The remainder of this work has been prepared in the following sections. The second section presents the geological setting of the Takht-e-Gonbad Porphyry Cu Deposit. In the third section, the electrical geophysics data is inverted in 2D along all profiles. In section four, the 3D models of electrical properties and Cu grade are constructed through geostatistical interpolation. In the fifth section, spatial correlation of the constructed geophysical models and Cu grade is discussed in details. Finally, all achievements are summarized in the conclusion section.

## 2. Geological setting of Takht-e-Gonbad porphyry Cu deposit

The Takht-e-Gonbad sulfide-content porphyry Cu deposit, which is an active mine at the present time, is located 80 km NE of Sirjan, Kerman Province,central domain of Iran. From the geological viewpoint, the Takht-e-Gonbad is a part of a wide mineralization belt named the Urmia-Dokhtar magmatic assemblage (UDMA), shown in Figure1. This area is covered by volcanic-pyroclastic units of Eocene age with dominant NE-

SW trends (Figure 2a). Volcanic tuff units host the Cu mineralization, as reported by the Yugoslavian geologists in the 1970s [34]. The mineralization and alteration zones are associated with Miocene granodiorite intruding the Eocene volcanic-pyroclastic rocks. The mineralization occurs as veins, veinlets, and disseminations in thermally metamorphosed and skarnized pyroclastic rocks as well as porphyritic intrusions [35, 36].

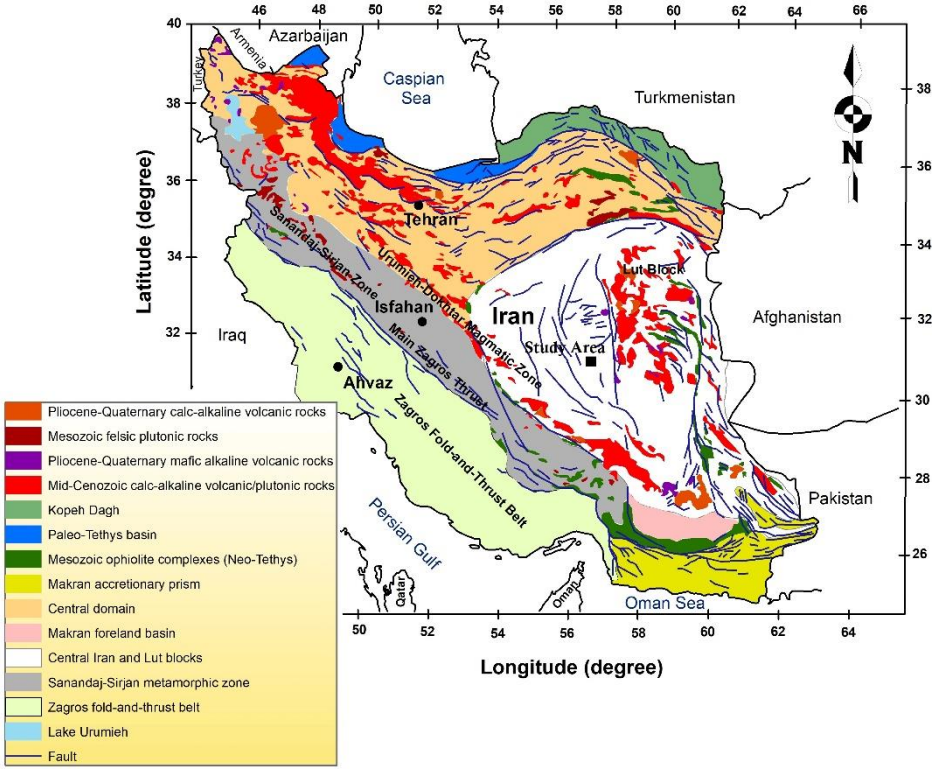


**Figure 1. Structural Geology map of Iran, where the location of the studied region is presented at the central portion over the Central Iran Block zone (reproduced with the permission of Richards *et al.* 2006).**

Phyllic, propylitic, silicic, and carbonate are the most significant alterations in the studied area. Phyllic alteration is more widespread and intensive over the tuffs and micro-granodiorite intrusions. In addition, this alteration is associated with copper mineralization in the hypogene zone. The major occurred minerals related to the phyllic alteration are sericite (muscovite, illite), quartz, subordinate chlorite, pyrite, and chalcopyrite [35]. Argillic or intermediate argillic alteration is the most extensive and the most common type of alteration for many porphyry-type Cu-bearing mineralization systems (e.g. [37, 38]). This alteration mostly occurs due to the alteration of plagioclase with the presence of the minerals, namely kaolinite, illite, smectite, and montmorillonite. In the studied area, the argillic alteration is widespread at the surface exposures and at shallow depths. Propylitic alteration occurs along the irregular zones characterized by variable chlorite, calcite, epidote and lower amounts of zeolite, and amphibole in this region [35, 36].

Chalcopyrite is the main mineral in the hypogene ore zone of the Takht -e-Gonbad deposit, exhibiting pyrite and minor magnetite along veins, and is found spreading over the granodiorite and tuff units. The economic grade of the hypogene ore has been detected about 150 m below the oxide cap [39, 40]. Note that in the oxide zone, chalcopyrite was converted to copper carbonate such as malachite. In the studied area, some of the mineralized parts are developed as transitional zones of immature supergene, hypogene, and oxide. The thickness of the enriched supergene zone is 10-50 m, characterized mainly by chalcocite and covellite [39, 41]. The studied area lies within an active tectonic setting, where most of the lineaments in the Takhte-e- Gonbad deposit are of dextral strike-slip type cut by the Nain-Baft and Chahar Gonbad faults in the south portions. The geological evidences indicate that mineralization has occurred mostly with an E-W strike [36, 41].

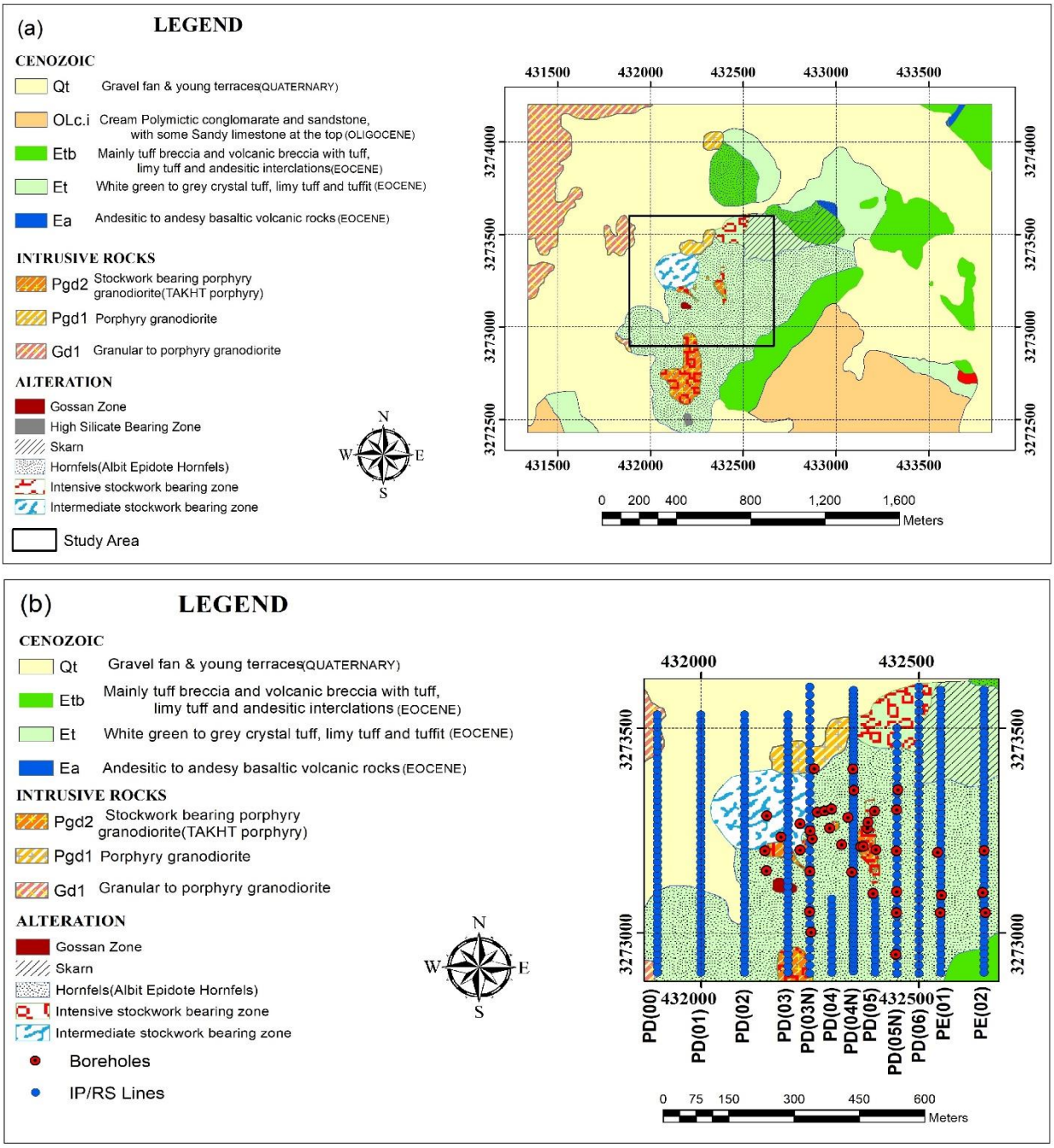


**Figure 2. Location and geology map of the Takht-e-Gonbad porphyry Cu deposit (a) on which 2D electrical tomography profiles and drilled boreholes have been superimposed (b).**

## 3. Geophysical survey

As noticed above, this work was carried out in order to investigate the efficiency of the electrical survey in the Takht-e-Gonbad porphyry Cu deposit. According to the direction and nature of mineralization observed in the outcrops, twelve electrical profiles were designed and surveyed through an instrument named Scintrex IPR12. Figure 2b shows a subset map of the geology on which the layout of the electrical survey and drillings has been superimposed. The profiles were designed along an N-S direction. The pole-dipole array configuration was chosen for data acquisition according to the depth of mineralization and surveying conditions. Such an electrical array can access a greater depth of investigation, leading to a more efficient field operation and also a high rate of data collection. The approach developed by Loke (2004) [33] was run to invert all the 2D electrical profiles.

From west to east of the studied area, the electrical profiles were named as PD00, PD01, PD02, PD03, PD03N, PD04, PD04N, PD05, PD05N, PD06, PE01, and PE02, respectively. PD04N was

surveyed on the main ore body, while its induced polarization (IP) data had an acceptable quality for modeling but unfortunately, its low-quality resistivity data was excluded from inversion. All the other profiles contained high quality Res and IP data. The PD00-PD03N profiles had a spacing of 100 m, PD03N-PE01 were 50 m apart, and finally, the spacing between PE01 and PE02 was about 100 m. The electrode spacing of PD00-PD03, PD04, PD05, and PE01-PE02 was about 30 m; PD03N, PD05N, and PE06 was 40 m, and finally, PD04N was 10 m. The profiles PD00-PD02 did not cross the boreholes but the rest of the profiles, less and more, covered the boreholes. Figure 3 indicates the 3D visualization of all the forty drilled holes in the area on which a relief topography map had been superimposed. The statistical summaries of all drillings (last row) were tabulated in Table 1.

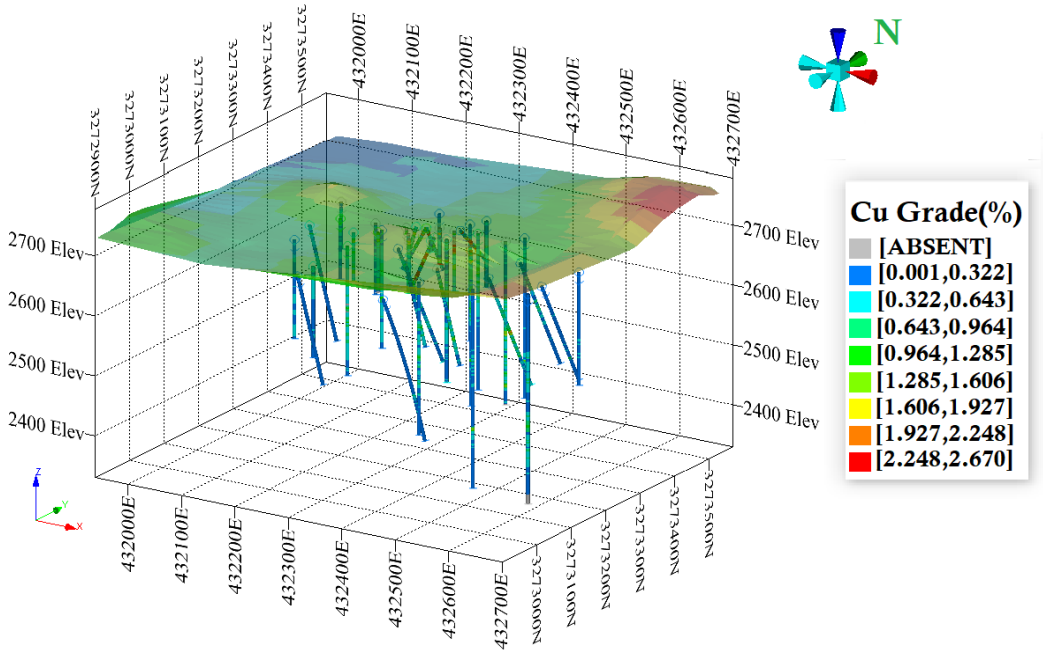


**Figure 3. Location map of boreholes with topography surface in the studied region, where the sulfide-content Cu grade has been inserted along each drilling.**

**Table 1. Statistical summary of the drilled boreholes.**

| Data set | Data count | Mean | Variance | Max. | Upper quartile | Median | Lower quartile | Min. |
|---|---|---|---|---|---|---|---|---|
| Res ($\Omega m$) | 5690 | 134.537 | 22142.9 | 2649.7 | 166.85 | 82.74 | 47.11 | 4.8 |
| IP (ms) | 7129 | 23.104 | 257.569 | 152.52 | 30.28 | 19.89 | 11.64 | 0.0019 |
| Cu (%) | 3340 | 0.3962 | 0.1484 | 2.57 | 0.54 | 0.3072 | 0.1244 | 0.0014 |

All the twelve electrical profiles were inverted iteratively in 2D through the least-squares method proposed by Loke (2004) [33] such that the recovered models could closely predict the apparent electrical data, i.e. generating an appropriate level of data misfit. All profiles were stitched together and presented in Figures 4a and 4b for electrical resistivity and chargeability, respectively. For a better interpretation of the models, the profile PD05N was chosen as a representative of all profiles, where five exploratory boreholes had crossed it (Figure 5). As it can be seen, the regions with a higher grade of Cu mineralization are spatially correlated with high values of the electrical resistivity and chargeability, respectively. Such geophysical signatures are usually common in the disseminated nature of Cu-bearing mineralization. In the following section, these physical properties are propagated in 3D through running a geostatistical approach to construct the geometry of the main source of mineralization.

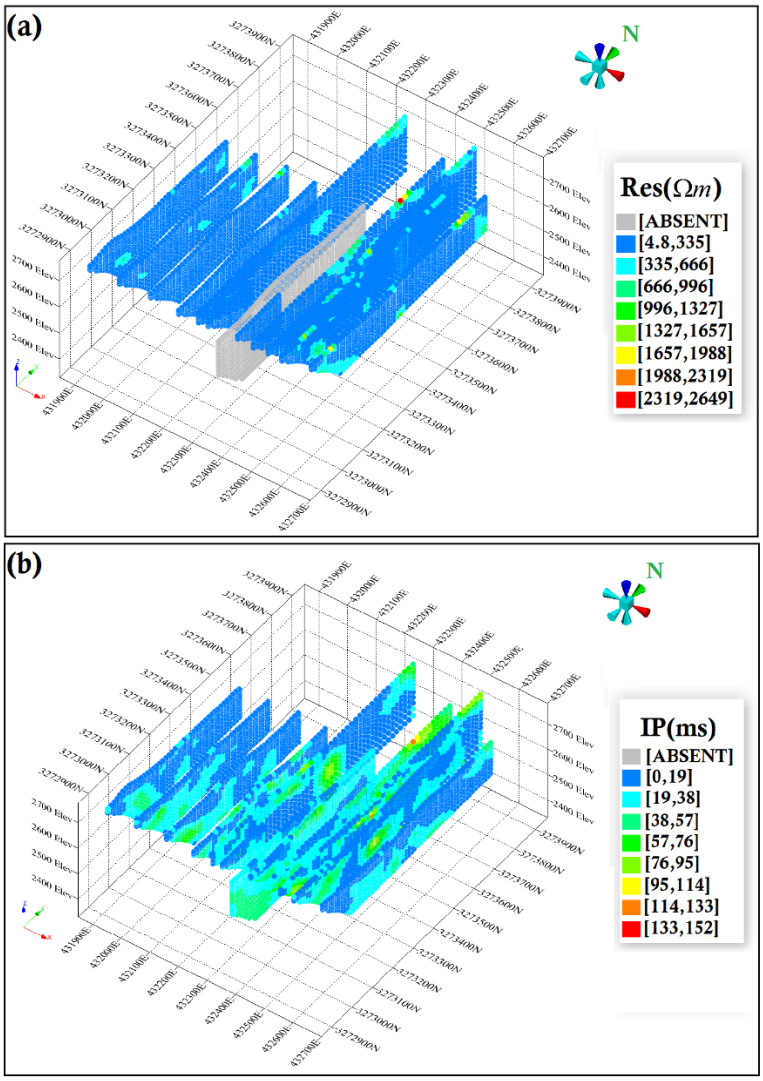


**Figure 4. 3D visualization of all 2D inverted profiles of electrical resistivity (a) and chargeability (b).**

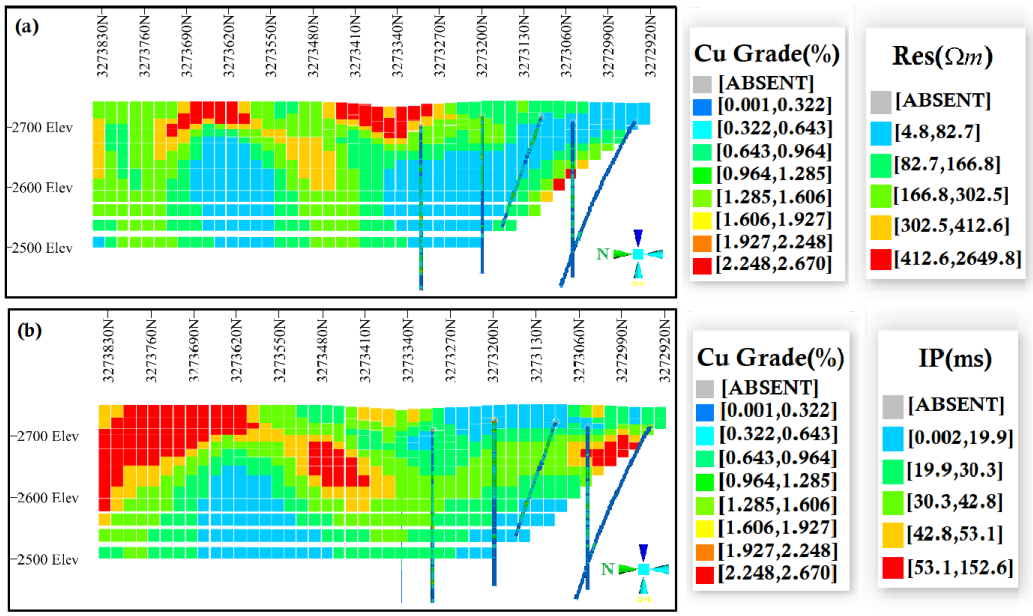


**Figure 5. A cross-section view of 2D inverted models of the electrical resistivity (a) and the induced chargeability (b) along profile PD05N, where the Cu grade along the drilled boreholes in adjacency to the electrical survey was superimposed on the section.**

## 4. Geostatistical models

In geostatistics, a spatial structure is essential for implementing the methods. The variogram is a fundamental tool in geostatistics for investigating the spatial structure. As it provides critical parameters for various Kriging estimators, the accuracy of the proposed parameters for the variogram is of crucial importance, and it can have a significant positive or negative influence on the estimated blocks [24]. The variogram provides a lot of information about the variables under study that are essential for all geostatistical calculations. One of the possible (and perhaps most important) uses of the variogram is the estimation of the variable value at the unsampled location and/or estimation of the average over a certain area [42]. The variogram is used to determine the spatial relationship between the regional variables, and is particularly attractive for geoscience engineering because the spatial characteristics of the studied region (e.g. range, anisotropy, and continuity) can be calculated [7].

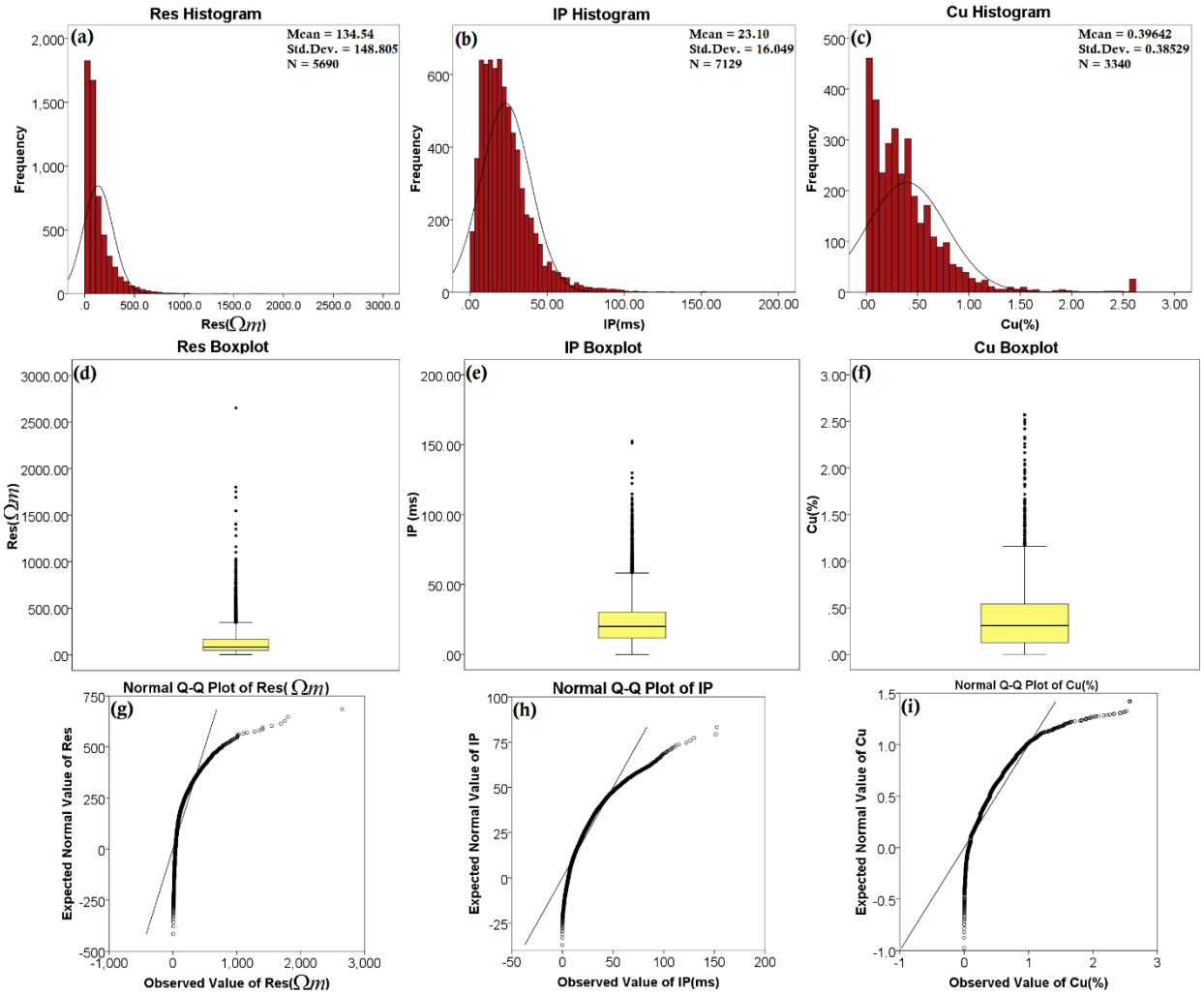


**Figure 6. The statistical charts that are histogram plot, box-plot, and q-q plot for the electrical resistivity (left column), chargeability (middle column), and Cu grade (right column).**

In order to prepare a 3D model in the first stage, variography was done for the Res, IP, and Cu data. The statistical summaries of these variables are listed in Table 1. Figure 6 presents those statistical characteristics by plotting the histogram, boxplot, and quantile-quantal (q-q) plots of each variable, all indicating non-normal distributions in the studied region. According to the above factors and applying the related software such as SGeMS (Stanford Geostatistical Modeling Software) [43], the experimental variograms for data were calculated and examined for various parameters such as different azimuths and dip angles. The appropriate theoretical models based on the least square differences were fitted to the variogram. For geostatistical estimation, we need to search for three variograms perpendicular to each other that construct an ellipsoid for calculating the directional covariance models. The search radius in the x, y, and z directions is used based on the range of

variograms. Thus the theoretical and empirical models of the directional variograms for the maximum, median, and minimum ranges are presented in Figures 7, 8, and 9 for the three variables Res, IP, and Cu, respectively. The number of pairs was also superimposed on these plots for each lag distance. Assuming a spherical model, the main characteristics of all fitted variogram models are listed in Tables 2, 3, and 4, respectively, for the three variables [7].

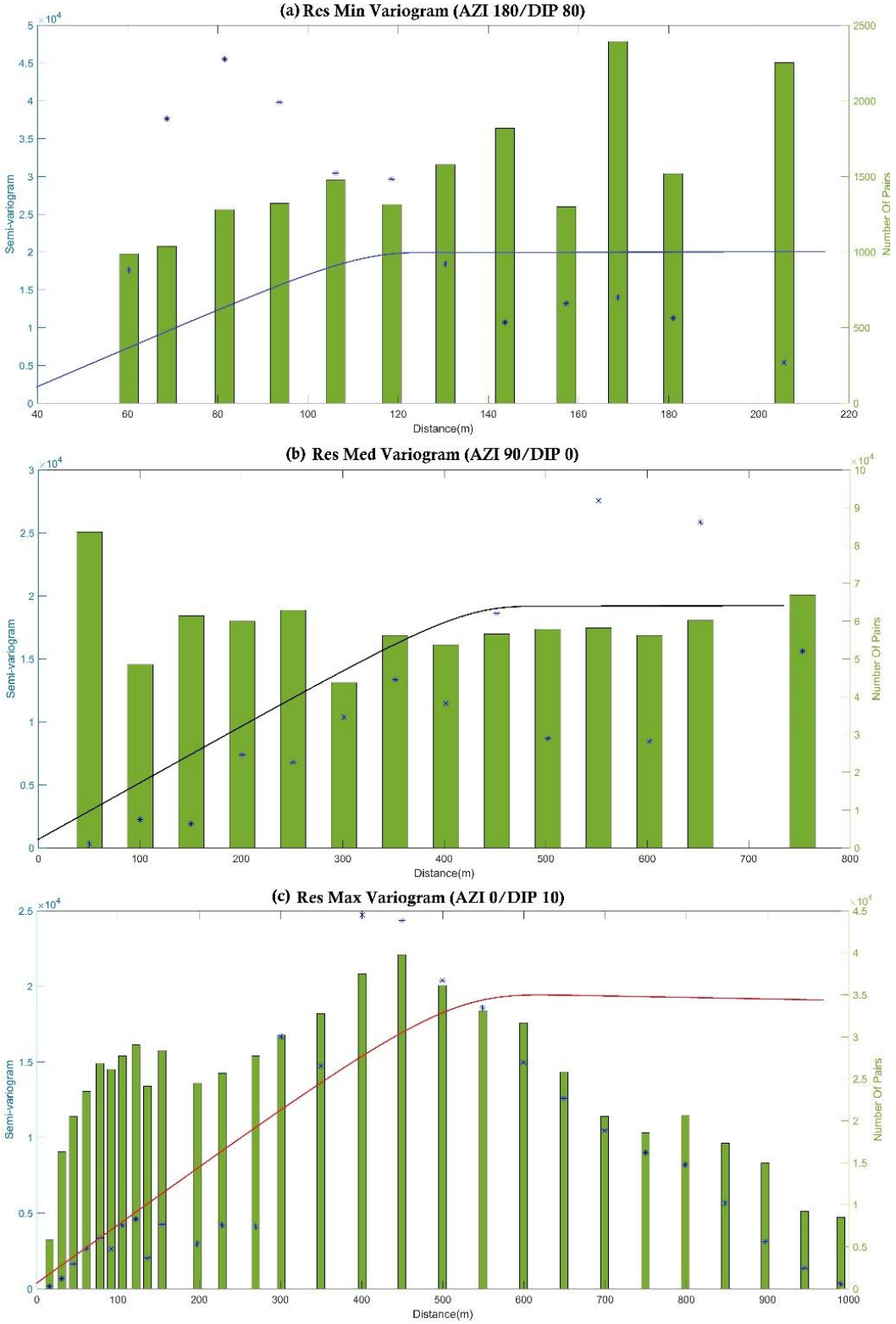


**Figure 7. Experimental directional semi-variogram, model, and number of pairs for the electrical resistivity along tri-axial with (a) minimum, (b) median, and (c) maximum range.**

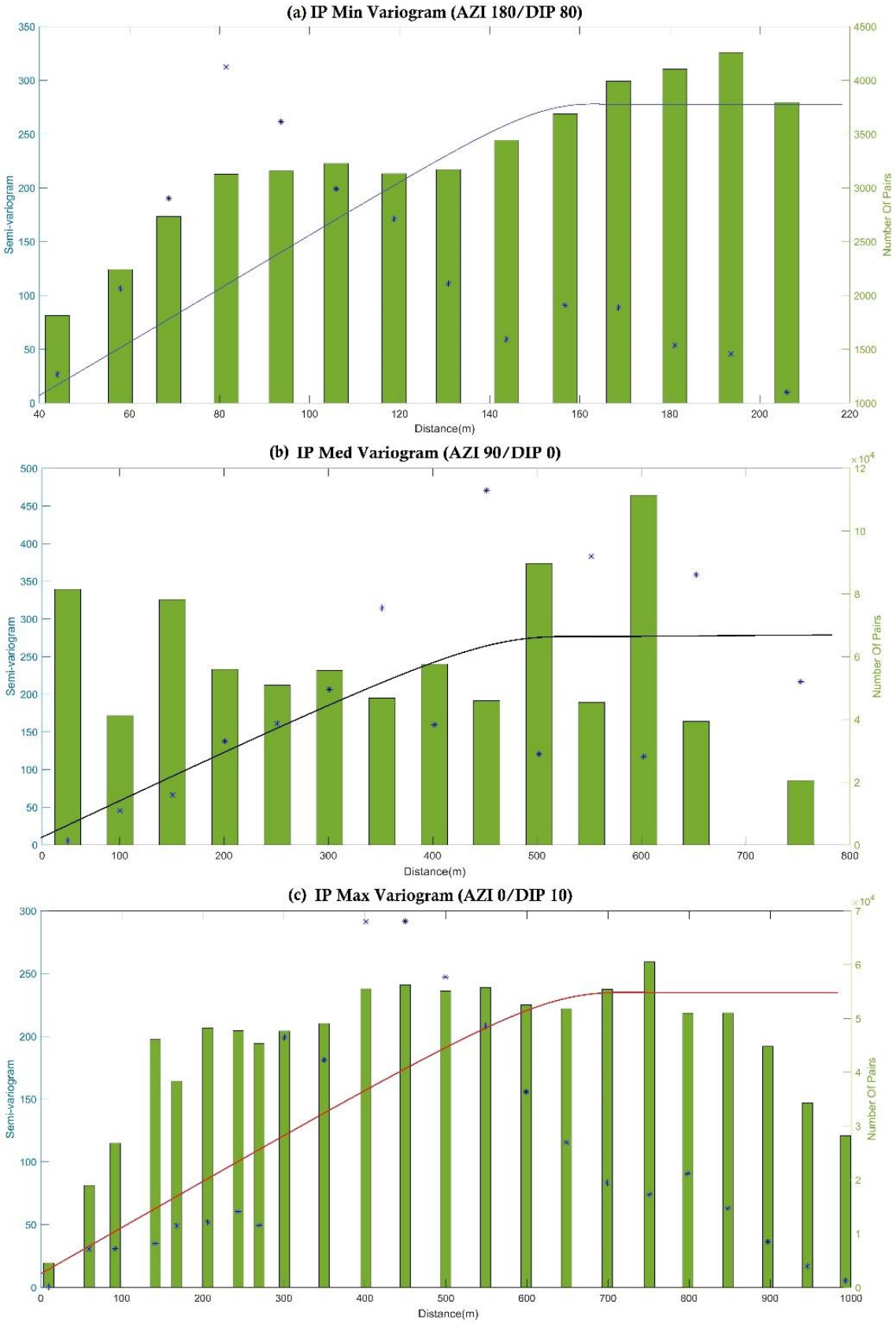


**Figure 8. Experimental directional semi-variogram, model, and number of pairs for the electrical chargability along tri-axial with (a) minimum, (b) median, and (c) maximum range.**

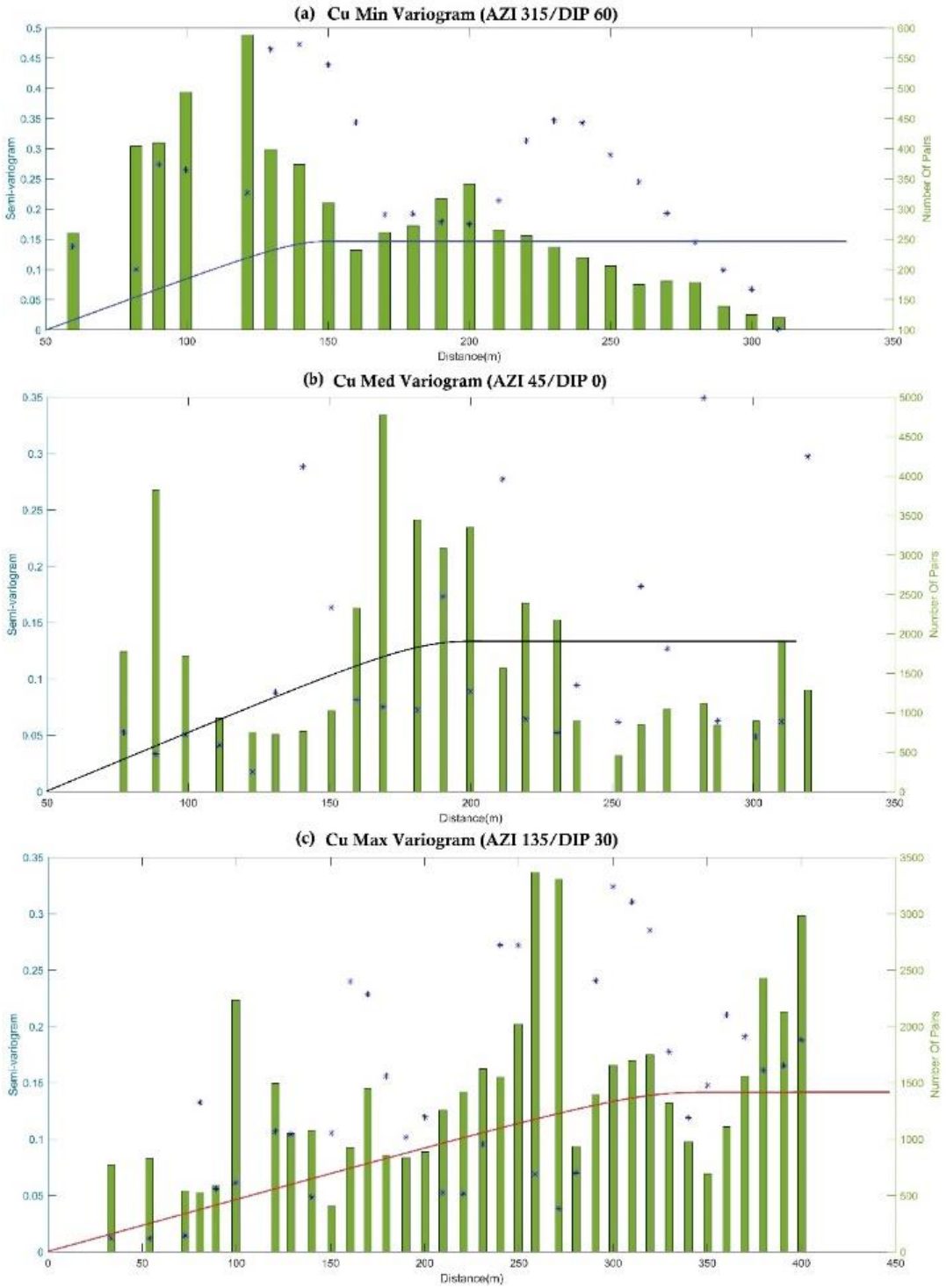


**Figure 9. Experimental directional semi-variogram, model, and number of pairs for the Cu distribution along tri-axial with (a) minimum, (b) median, and (c) maximum range.**

**Table 2. Parameters obtained for the variogram model of the electrical resistivity.**

| Major/Minor | Azimuth | Dip | Range | Sill | Nugget | Model |
|---|---|---|---|---|---|---|
| Maximum | 0 | 10 | 600.7 | 22391.7 | 2214.287 | Spherical |
| Median | 90 | 0 | 528.4 | 22391.7 | 2214.287 | Spherical |
| Minimum | 180 | 80 | 135.1 | 22391.7 | 2214.287 | Spherical |

**Table 3. Parameters obtained for the variogram model of the electrical chargeability.**

| Major/Minor | Azimuth | Dip | Range | Sill | Nugget | Model |
|---|---|---|---|---|---|---|
| Maximum | 0 | 10 | 716.1 | 260 | 25.757 | Spherical |
| Median | 90 | 0 | 495.7 | 260 | 25.757 | Spherical |
| Minimum | 180 | 80 | 175.7 | 260 | 25.757 | Spherical |

**Table 4. Parameters obtained for the variogram model of the Cu grade.**

| Major/Minor | Azimuth | Dip | Range | Sill | Nugget | Model |
|---|---|---|---|---|---|---|
| Maximum | 135 | 30 | 349.7 | 0.15 | 0.015 | Spherical |
| Median | 45 | 0 | 199.9 | 0.15 | 0.015 | Spherical |
| Minimum | 315 | 60 | 150.9 | 0.15 | 0.015 | Spherical |

After variogram fitting and obtaining the variogram parameters, determining the uncertainties of the fitted models is required. By the jackknife Kriging method [44], the variogram parameters are obtained and the uncertainties are determined. In the Jackknife analysis, the estimated data is compared against the measured values for a set of locations different from those used as the input data. The calculation of the difference between the measured values (experimental) and the estimated values in the same points by the Kriging method is introduced as the jackknife error. The average of this error should be zero, and the standard deviation of this error should be minimum [44]. The diagrams of the actual values against the estimated values for the three variables (i.e. Res, IP, and Cu) are presented in Figure 10 [7]. On the basis of the fitted linear curve between the actual and estimated values, acceptable Pearson's correlation coefficients were acquired. They were equal to 0.9021, 09689, and 0.8120 for Res, IP, and Cu, respectively. Since the drillings are a bit sparser compared to the electrical data, the correlation coefficient between the leave-out data and the actual ones is a bit lesser. Therefore, it can be deduced that the variogram parameters have a sufficient accuracy for 3D modeling of these variables.

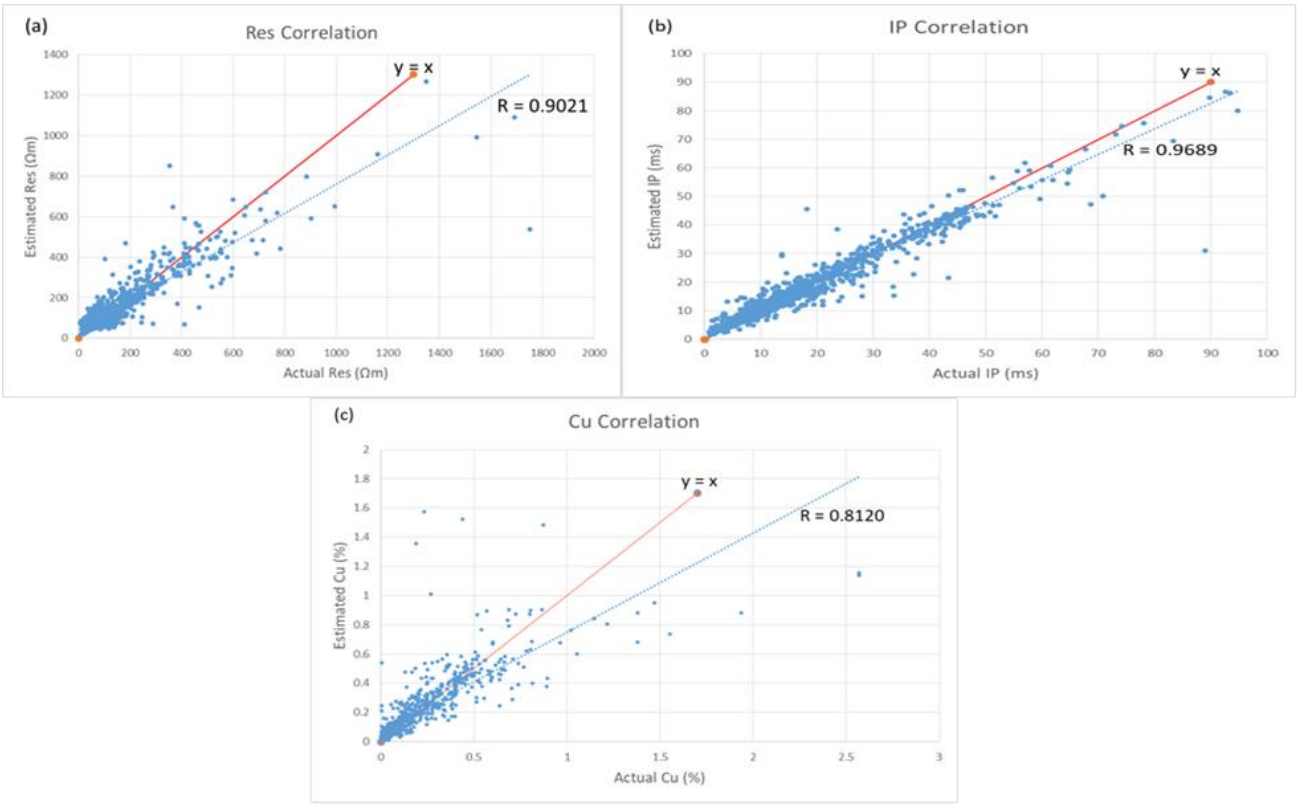


**Figure 10. Scatter plots of the actual values against the estimated leave-out data for the electrical resistivity (a), chargeability (b), and Cu sulfide (c).**

The electrical properties and Cu grade were interpolated in 3D by an ordinary Kriging algorithm, assuming the block sizes in the x, y, and z directions to be equal to 10, 10, and 5 m, respectively. Since various rock types and alterations often occur in the porphyry-type systems, we assumed a constant unknown mean only over the search neighborhood to deduce the ordinary Kriging system for the assumptions of the model. Figure 11 presents the volumes rendering these models by assuming the threshold values of 500 Ωm, 50 ms, and 0.4% of the Cu grade. These thresholds were determined by a trial-and-error test to find out the anomalous zones of the electrical models in association with the Cu mineralization. Notice that these geophysical models visually have a strong consistency in localizing Cu mineralization. There is a dominant anomaly in the studied area with an almost W-E strike. The depth of mineralization in the northern part is more than that in the southern part. The average thickness of the mineral body is about 80 m as well.

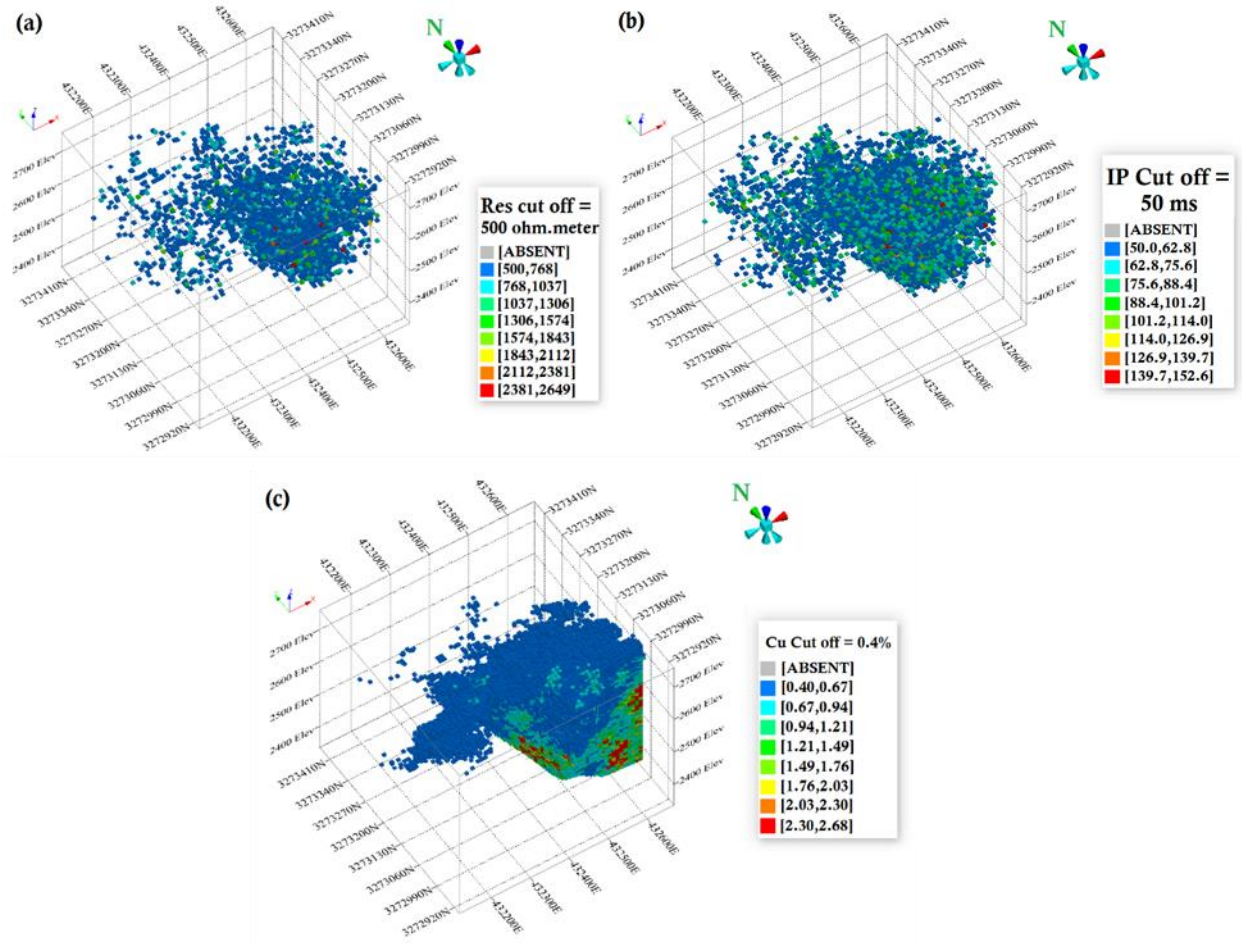


**Figure 11. 3D models of the electrical resistivity (a), chargeability (b), and Cu grade in the studied region for cut-off values of 500 Ωm, 50 ms, and 0.4%, respectively.**

The Kriging estimation variance (EV) is a measure of uncertainty in predictions, and is a function of the variogram, sample structure, and sample support (the area in which an observation is made, which may be estimated as a point or may be an area) [45]. Evaluating EV in each point, which is not dependent on the data value, is one of the main strengths of the geostatistical methods. Moreover, Kriging gives an error distribution as well. The estimation variances of the Res, IP and Cu data were calculated and presented in 3D block models in Figures 12a, 12b, and 12c, respectively. Due to the normalization of data, the estimation variance value lies between 0 and 1. The minimum value for the EV indicates that the error of estimation is minimum, and with an increase in the amount of the EV error, the value of estimation and modeling increase. The results obtained show that the minimum variance is in the profile location, and away from the profiles, the estimation variance is increased [7].

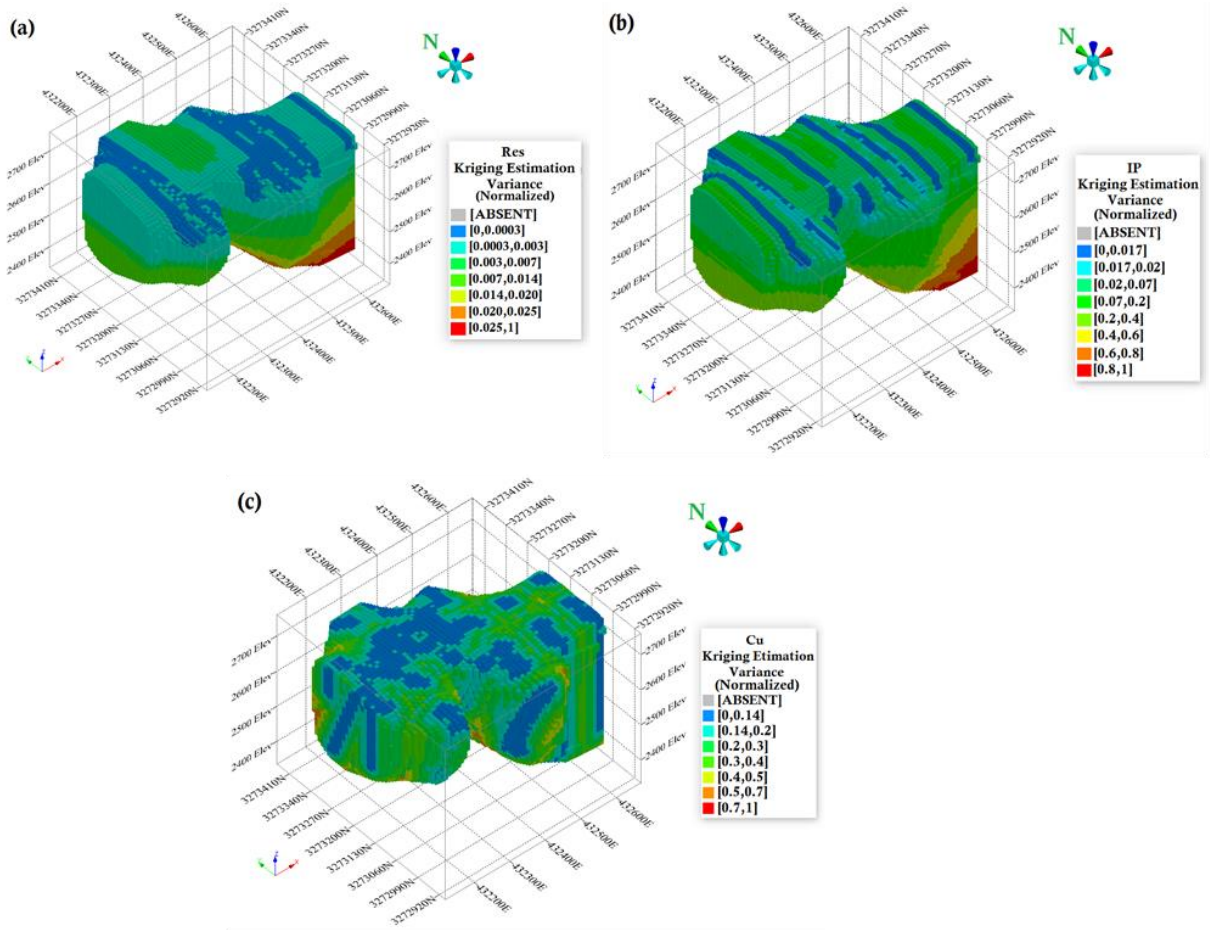


**Figure 12. 3D uncertainty visualization of the electrical resistivity (a), chargeability (b), and Cu grade models acquired from the ordinary Kriging.**

## 5. Discussion

Field surveying and data acquisition were done successfully. The data obtained was revised, the accuracy was checked, and then processing was carried out. In the first stage, 2D imaging of the electrical properties along twelve profiles was generated through running a 2D inversion algorithm. Therefore, the 3D models of the desired variables (i.e. physical properties and Cu grade) were prepared based on a geostatistical method. The results of 3D modeling were successfully checked by the geostatistical methods and the drilling results.

Figure 13 shows the pairwise correlation of each model versus the others, where a positive coefficient exists in all plots. According to the results obtained from the geophysical study and the one from the drilling data, we can say that the Res and IP sections and the mineralized zones have a rather well agreement with each other. Location of the Cu mineralization is traced with an acceptable accuracy by high values of both the Res and IP properties. In resource modeling, the importance of the non-mineralized zone separation is as much as those mineralized zones, where the employed 2D electrical profiles have surveyed all of these regions (i.e. non-mineralized and mineralized) to localized favorable zones of mineralization in adjacency to the non-mineralized zones. Note that the geophysical properties are indirectly correlated to the Cu grade, and lots of ambient factors and data modeling can affect the geophysical results, which lead to the partial correlation of these variables. We believe that those acquired correlation coefficients are genuinely meaningful between the physical properties and the Cu grade (i.e. 0.41 and 0.49, respectively, for the Res and IP values versus the Cu grade). The importance of these scatter plots can be projected in Figure 11, where the geometry of Cu-bearing zones is closely in association with those arising from the electrical survey.

A combination of the drilling and inversion results leads to reveal two main lithology types including the sedimentary and igneous units. The sedimentary units include sandstone and limestone with marl and shale, detected by a low Res value (less than 300 Ωm). The igneous rock includes tracchy-andesite and porphyritic andesite, determined by a high Res value (more than 300 Ωm) that have been considered as the host-rocks of the mineralization. The copper mineralization is related to the high IP values. The efficiency of the IP and Res models in the Takht-e-Gonbad Porphyry Cu Deposit is rather high, and using this investigation can reduce and optimize the drilling operation for resource estimation.

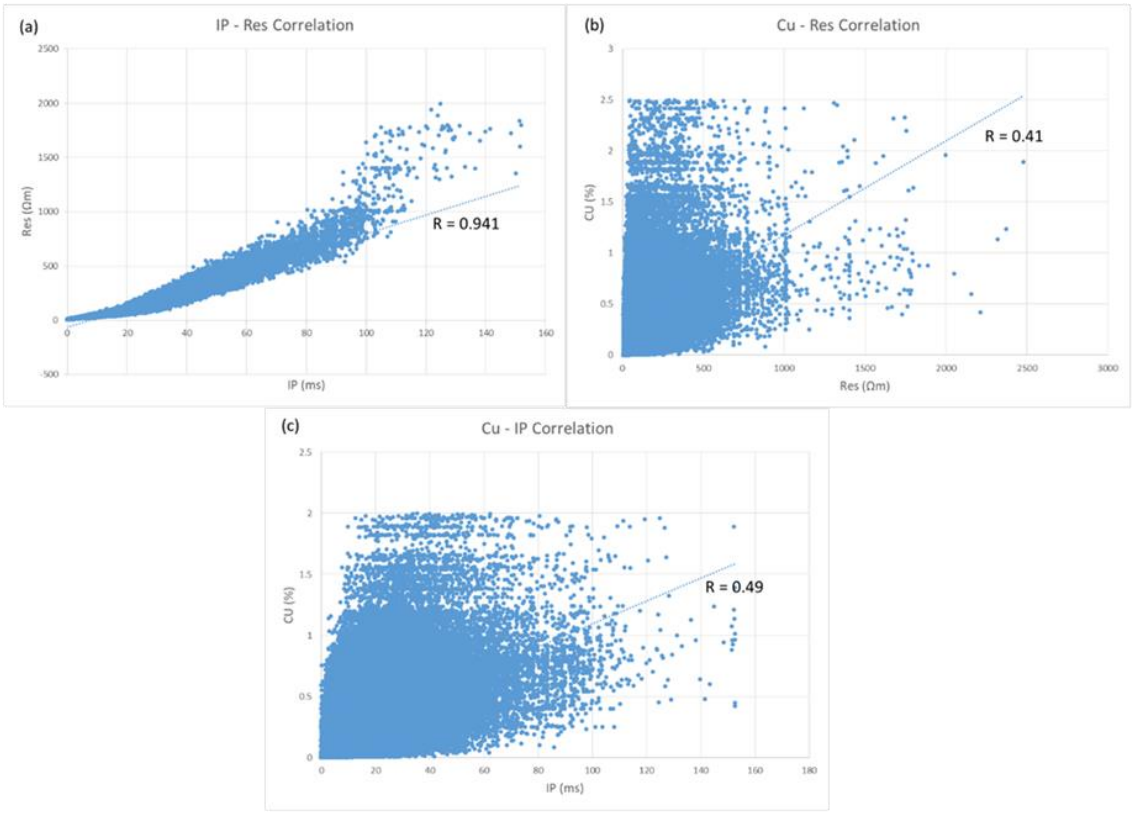


**Figure 13. Scatter plots between (a) RS-IP, (b) RS-Cu, and (c) IP-Cu. Pearson's correlation coefficient between each model has been calculated.**

## 6. Conclusions

The time-domain induced polarization (IP) and DC-resistivity (Res) have been successfully used in order to delineate the mineralized zones in the Takht-e-Gonbad Porphyry-Cu Deposit. The 2D models of the electrical resistivity and chargeability along twelve profiles were generated to be interpolated in 3D through a geostatistical approach. The anomalous geophysical zone extracted from the 3D models of the electrical properties had a good conformity with the E-W strike of copper mineralization in the region, where tracchy-andesite and porphyritic andesite hosted the main body of mineralization. Note that higher values of both electrical models were in association with a higher grade of Cu mineralization, proving a dominant disseminated nature of copper mineralization in the area. Such correlated geophysical models could generate valuable insights into the second phase of exploration program for designing the layout of further exploratory drillings and constructing the geometry of the Cu deposit for resource estimation when a sparse pattern of drilling exists.

**Acknowledgements**

The authors wish to appreciate the Geophysics Lab of the School of Mining Engineering, the University of Tehran, for providing the facilities to process and model the geophysical data. We also wish to thank the Editor-in-Chief of the Journal of Mining and Environment, Prof. Ataei, and the two anonymous referees for reviewing the paper precisely and patiently, and for their constructive and valuable comments, which helped us to improve the quality of this work.

## References

[1]. Gadallah, M.R. and Fisher, R. (2009). Exploration Geophysics. Berlin. Springer. http://doi.org/ 10.1007/978-3-540-85160-8.

[2]. Telford, W.M., Geldart, L.P. and Sheriff, R.E. (1990). Applied Geophysics. Cambridge. Cambridge University Press. http://doi.org/10.1180/minmag. 1982.046.341.32.

[3]. Ramazi, H. and Mostafaie, K. (2013). Application of integrated geoelectrical methods in Marand (Iran) manganese deposit exploration. Arabian Journal of Geosciences. 6 (8): 2961-2970.

[4]. Mostafaie, K. and Ramazi, H. (2015). Application of electrical resistivity method in sodium sulfate deposits exploration, case study: Garmab, Iran. Journal of Biodiversity and Environmental Sciences. 6 (2): 2220-6663.

[5]. Sultan, S.A., Mansour, S.A., Santos, F.M. and Helaly, A.S. (2009). Geophysical exploration for gold and associated minerals, case study: Wadi El Beida area, South Eastern Desert, Egypt. Journal of Geophysics and Engineering. 6 (4): 345-356.

[6]. Ferdows, S.M. and Ramazi, H. (2015) Application of the fractal method to determine the membership function parameter for geoelectrical data (case study: Hamyj copper deposit, Iran). Journal of Geophysics and Engineering. 12 (1): 909-921.

[7]. Mostafaei, K., Ramazi, H. (2018). 3D model construction of induced polarization and resistivity data with quantifying uncertainties using geostatistical methods and drilling (Case study: Madan Bozorg, Iran). Journal of Mining and Environment. 9(4): 857-872. doi: 10.22044/jme.2018.6852.1516.

[8]. Yang, J., liu, Z.H. and Wang, L. (2008). Effectiveness of Natural Field Induced Polarization for Detecting Polymetallic Deposits. Earth Science Frontiers. 15 (4): 217-221.

[9]. Cardarelli, E., Di Filippo, G., 2009. Electrical resistivity and induced polarization tomography in identifying the plume of chlorinated hydrocarbons in sedimentary formation: a case study in Rho (Milan - Italy). Waste Management & Research. 27: 595-602.

[10]. Flores, C. and Peralta-Ortega, S.A. (2009). Induced polarization with in-loop transient electromagnetic soundings: A case study of mineral discrimination at El Arco porphyry copper, Mexico. Journal of Applied Geophysics. 68 (3): 423-436.

[11]. Daneshvar Saein, L., Rasa, I., Rashidnejad Omran, N., Moarefvand, P. and Afzal, P. (2012). Application of concentration-volume fractal method in induced polarization and resistivity data interpretation for Cu-Mo porphyry deposits exploration, case study: Nowchun Cu-Mo deposit, SE Iran. Nonliner Processes in Geophysics. 19: 431-438.

[12]. Kozhevnikov, N.O., Antonov, E.Y., Zakharkin, K. and Korsakov, M. (2014). TEM surveys for search of taliks in areas of strong fast-decaying IP effects. Russian Geology and Geophysics. 55 (12): 1452-1460.

[13]. Madun, A., Tajudin, S.A.A., Sahdan, M.Z., Dan, M.F.M., Talib, M.K.A. (2018). Electrical resistivity and induced polarization techniques for groundwater exploration. International Journal of Integrated Engineering. 10(8): 56-60.

[14]. Gurin, G., Tarasov, A., Ilyin, Y. and Titov, K. (2015). Application of the Debye decomposition approach to analysis of induced-polarization profiling data (Julietta gold-silver deposit, Magadan Region). Russian Geology and Geophysics. 56: 1757-1771.

[15]. Mashhadi, S.R., Mostafaei, K. and Ramazi, H.R. (2017). Improving bitumen detection in resistivity surveys by using induced polarization data. Exploration Geophysics. Published online: https://doi.org/ 10.1071/EG17032.

[16]. Doulati Ardejani, F., Jodeiri Shokri, B., Moradzadeh, A., Soleimani, E. and Jafari, M.A. (2008). A combined mathematical geophysical model for prediction of pyrite oxidation and pollutant leaching associated with a coal washing waste dump. International Journal of Environmental Science and Technology. 5 (4): 517-526.

[17]. Rucker, D.F., Glaser, R.D., Osborne, T. and Maeh, W. (2009). Electrical Resistivity Characterization of a Reclaimed Gold Mine to Delineate Acid Rock Drainage Pathways. Mine Water Environment. 28: 146-157.

[18]. Gomez, E.P., Parviainen, A., Hokkanen, T. and Ruskeeniemi, K.L. (2010). Integrated geophysical and geochemical study on AMD generation at the Haveri Au-Cu mine tailings, SW Finland. Environmental Earth Science. 1: 1435-1447.

[19]. Jodeiri Shokri, B., Doulati Ardejani, F. and Moradzadeh, A. (2016). Mapping the flow pathways and contaminants transportation around a coal washing plant using the VLF-EM, Geo-electrical and IP techniques-A case study, NE Iran. Environmental Earth Sciences. 75 (1): 1-13.

[20]. López-González, A.E., Tejero-Andrade, A., Hernández-Martínez, J.L., Prado, B., Chávez, R.E., (2019). Induced Polarization and Resistivity of Second Potential Differences (spd) with Focused Sources Applied to Environmental Problems. Journal of Environmental and Engineering Geophysics. 24 (1): 49–61.

[21]. Mashhadi, S.R. Ramazi, H. (2018). The Application of Resistivity and Induced Polarization Methods in Identification of Skarn Alteration Haloes: a Case Study in the Qale-alimoradkhan Area. Journal of Environmental and Engineering Geophysics. 23 (3): 363-368.

[22]. Gazoty, A., Fiandaca, G., Pedersen, J., Auken, E., Christiansen, A.V., Pedersen, J.K. and Syddanmark, R. (2012). Application of time domain induced polarization to the mapping of lithotypes in a landfill site. Hydrology and Earth System Science. 16: 1793-1804.

[23]. Bourges, M., Mari, J. and Jeann, N. (2012). A practical review of geostatistical processing applied to geophysical data: methods and applications. Geophysical Prospecting. pp. 1-13. doi: 10.1111/j.1365-2478.2011.00992.x.

[24]. Mostafaie, K., Ramazi, H. and Jalali, M. (2014). Application of Integrated Geophysical and Geostatistical Methods in Amiriyeh Site Classification. Geodynamics Research International Bulletin (GRIB). 2 (2): 1-15.

[25]. Kumar, D., Ahmed, S., Krishnamurthy, N.S. and Dewandel, B. (2007). Reducing ambiguities in vertical electrical sounding interpretations: A geostatistical application. Journal of Applied Geophysics. 62 (1): 16-32.

[26]. Vesnaver, A., Bridle, R., Henry, B., Ley, R., Rowe, R. and Wyllie, A. (2006). Geostatistical integration of near-surface geophysical data. Geophysical Prospecting. 54 (6): 763-777.

[27]. Morari, F., Castrignano, A. and Pagliarin, C. (2009). Application of multivariate geostatistics in delineating management zones within a gravelly vineyard using geo-electrical sensors. Computers and Electronics in Agriculture. 68 (1): 97-107.

[28]. Huang, J., Zhao, B., Chen, Y. and Zhao, P. (2010). Bidimensional empirical mode decomposition (BEMD) for extraction of gravity anomalies associated with gold mineralization in the Tongshi gold field, Western Shandong Uplifted Block, Eastern China. Computers and Geosciences. 36 (7): 987-995.

[29]. Ramazi, H. and Jalali, M. (2014). Contribution of geophysical inversion theory and geostatistical simulation to determine geoelectrical anomalies. Studia Geophysica et Geodaetica. 59 (1): 97-112.

[30]. Abedi, M., Asghari, O., Norouzi, G.-H., (2015). Collocated cokriging of iron deposit based on a model of magnetic susceptibility: a case study in Morvarid mine, Iran. Arabian Journal of Geosciences. 8 (4): 2179-2189.

[31]. Asghari, O., Sheikhmohammadi, S., Abedi, M., Norouzi, G., (2016). Multivariate geostatistics based on a model of geo-electrical properties for copper grade estimation: a case study in Seridune, Iran. Bollettino di Geofisica Teorica ed Applicata. 57(1).

[32]. Salarian, S., Asghari, O., Abedi, M., Alilou, S. K., (2019). Geostatistical-based geophysical model of electrical resistivity and chargeability to image Cu mineralization in Ghalandar deposit, Iran. International Journal of Mining Geo-Engineering (in press).

[33]. Loke, M., 2004. Tutorial: 2-D and 3-D electrical imaging surveys.

[34]. Geological Survey of Iran. (1973). Exploration for Ore Deposits in Kerman Region. Rep. Yu/53 (247 pp.).

[35]. Hosseini, M.R., Ghaderi, M. Alirezaei, S. and Sun, W. (2017). Geological characteristics and geochronology of the Takht-e-Gonbad copper deposit, SE Iran: a variant of porphyry type deposits. Ore Geol. Rev. 86, 440e458. https://doi.org/10.1016/j.

[36]. Mohammadi, N.M., and Hezarkhani, A. (2018). Application of support vector machine for the separation of mineralised zones in the Takht-e-Gonbad porphyry deposit, SE Iran. Journal of African Earth Sciences. 143: 301-308.

[37]. Ranjbar, H., Honarmand, M., and Moezifar, Z. (2004). Application of the Crosta technique for porphyry copper alteration mapping, using ETMþ data in the southern part of the Iranian volcanic sedimentary belt. J. Asian Earth Sci. 24: 237e243.

[38]. Alirezaei, S., and Hassanpour, S. (2011). An overview of porphyry copper deposits in Iran. In: The 1st World Copper Congress, Iran. Proceedings with Abstracts. pp. 49e62.

[39]. Hosseini, M.R. (2012). Mineralogy, Geochemistry, Fluid Inclusion and Genesis of Takht-e-Gonbad Copper Deposit. Northeast Sirjan (M.Sc. thesis). Tarbiat Modares University, Tehran, Iran. 257 pp. (in Persian with English abstract).

[40]. Afzal, P., Tehrani, M.E., Ghaderi, M., and Hosseini, M.R., (2016). Delineation of supergene enrichment, hypogene and oxidation zones utilizing staged factor analysis and fractal modeling in Takht-e-Gonbad porphyry deposit, SE Iran. J. Geochem. Explor. 161: 119e127.

[41]. Hosseini, M.R., Ghaderi, M., and Alirezaei, S. (2011). Geology, alteration and mineralization characteristics of Takht-e-Gonbad copper deposit, northeast Sirjan. In: Proceedings of the 1st World Copper Congress, Tehran, Iran, pp. 160e170 (in Persian with English abstract).

[42]. Zawadzki, J. and Fabijańczyk, P. (2007). Use of variograms for field magnetometry analysis in Upper Silesia Industrial Region. Studia Geophysica et Geodaetica. 51(4): 535-550

[43]. Bohling, G. (2007). S-GeMS Tutorial Notes in Hydrogeophysics: Theory, Methods, and Modeling, Boise State University, Boise, Idaho.

[44]. Lamorey, G. and Jacobson, E. (1995). Estimation of Semivariogram Parameters and Evaluation of the Effects of Data Sparsity. Mathematical Geology. 27 (3): 327-358.

[45]. Journel, A.G. and Huijbregts, C.H.J. (1978). Mining Geostatistics, Centre de Geostatistique Fontainebleau. France.

# مدل‌سازی زمین‌آماری توموگرافی مقاومت الکتریکی جهت تصویرسازی کانه‌زایی مس پورفیری نهشته تخت‌گنبد ایران

**محمود بابایی، میثم عابدی*، غلامحسین نوروزی، سعید کاظم علیلو**

**دانشکده مهندسی معدن، پردیس دانشکده‌های فنی، دانشگاه تهران، ایران**

ارسال ۲۰۱۹/۷/۱۷، پذیرش ۲۰۱۹/۱۰/۲۶

* نویسنده مسئول مکاتبات: maysamabedi@ut.ac.ir

**چکیده:**

در این تحقیق، کاربرد یک رهیافت مدل‌سازی مبتنی بر زمین‌آمار برای ساختن ویژگی‌های الکتریکی منتج از برداشت ژئوفیزیکی توموگرافی الکتریکی جهت اکتشاف نهشته مس پورفیری تخت گنبد در ایران مرکزی تشریح می‌شود. داده‌های الکتریکی به صورت دوبعدی در امتداد چند پروفیل بر روی زون‌های با پتانسیل بالای کانه‌زایی مس، وارون سازی می‌شوند تا ویژگی‌های مقاومت‌ویژه و بارپذیری الکتریکی تصویر شود. به‌دلیل همبستگی بالای فضائی ویژگی‌های ژئوفیزیکی و کانه‌زایی مس (عیار مس)، مدل‌های الکتریکی به صورت سه‌بعدی از روی درون‌یابی زمین‌آماری داده‌های وارون شده دوبعدی ساخته می‌شوند تا شمای کلی در مورد هندسه کانه‌زایی احتمالی تهیه شود. زون بی‌هنجاری ژئوفیزیکی با مقادیر بالای مقاومت‌ویژه و بارپذیری الکتریکی منطبق با توده اصلی کانه‌زایی با عیار بالای مس حاصله از حفاری اکتشافی است. نتایج حاکی از این است که سیستم کانه‌زایی مس پورفیری در این ناحیه دارای شواهد ژئوفیزیکی قوی است که توسط دگرسانی‌ها و نوع سنگ‌ها کنترل می‌شوند. چنین مدل‌های فیزیکی اطلاعات با ارزشی جهت طراحی جانمایی حفاری‌های بیشتر اکتشافی، ساختن ویژگی‌های زمین‌شناسی، جدایش زون‌های غیر کانه‌زایی از کانه‌زایی و مدل‌سازی منبع تهیه می‌نمایند.

**کلمات کلیدی:** مقاومت الکتریکی، بارپذیری الکتریکی، زمین‌آمار، وارون‌سازی، مس پورفیری.